Raman scattering in polycrystalline 3*C*-SiC: Influence of stacking faults

Stefan Rohmfeld, Martin Hundhausen, and Lothar Ley
Institut für Technische Physik, Universität Erlangen-Nürnberg, Erwin-Rommel-Straße 1, D-91058 Erlangen, Germany
(Received 29 May 1998)

We report temperature dependent measurements of the Raman spectra of microcrystalline 3*C*-SiC free-standing films. The measurements were performed under direct laser heating of the thin films for temperatures up to 1700 K. The temperature dependence of the TO- and LO-phonon frequencies agrees well with that of single-crystal 3*C*-SiC, but the Raman lines are considerably broader. We discuss the influence of stacking faults on the linewidth by comparing our results with computer simulated Raman intensity profiles of 3*C*-SiC structures having randomly distributed stacking faults. Good agreement with respect to the linewidth and disorder-induced peak shift is found if the average stacking fault distance is assumed to be 6 Å. We observe an irreversible narrowing of the Raman lines at temperatures above 1900 K, which we ascribe to an annealing of stacking faults in 3*C*-SiC. [S0163-1829(98)08139-9]

I. INTRODUCTION

Silicon carbide (SiC) is a wide-band-gap semiconductor that crystallizes in a large number of polytypes. In all polytypes, each silicon atom is bonded tetrahedrally to four neighboring carbon atoms, and vice versa. The atoms are arranged in Si-C double layers, which are stacked on top of each other to form the crystal. There are two possible orientations of adjacent double layers which are rotated by 60° with respect to each other around the layer normal. One, where the bonds in the two layers are in an eclipsed configuration, as it is found in the wurtzite structure (2*H*-SiC), is called hexagonal. The other orientation (staggered), corresponding to the zinc-blende structure (3*C*-SiC), is called cubic. All other polytypes (4*H*,6*H*,15*R*, . . .) are constructed from particular sequences of hexagonal and cubic stacking orientations.

Wide band gaps between 2.2 eV (3*C*) and 3.3 eV (2*H*),[1] a high saturated electron drift velocity, and a high electric breakdown field[2] combined with a high thermal conductivity make silicon carbide a material suitable for electronic devices operating at high power, frequency, and temperature. For these applications it is important to characterize SiC at elevated temperatures and after thermal treatment. The different stacking sequences for each polytype are associated with a characteristic set of phonon modes at the Brillouin-zone center, and polytypes may thus be identified on the basis of these modes as measured by Raman spectroscopy.[3,4] The corresponding Raman intensity profiles have been calculated in a bond polarizability and linear chain model for various single crystalline SiC polytypes.[5–7] Calculations for a random mixture of two polytypes which is meant to represent one dimensionally—along the layer normal—disordered SiC exhibit broadened and distorted Raman bands.[8]

Here we study the influence of temperature on the frequencies and linewidths of the TO and LO Raman lines of microcrystalline 3*C*-SiC prepared by low-temperature chemical vapor deposition on silicon. The distinct differences to the Raman spectra of single-crystalline 3*C*-SiC (Ref. 9) are discussed with the aid of numerical simulations calculated using the bond polarizability concept and a linear chain model.

II. EXPERIMENTAL DETAILS

The silicon carbide films studied here were grown on Si(100) substrates to a thickness of 3 μm by chemical vapor deposition[10] at temperatures of about 1350 K. The growth condition were intentionally chosen in such a way as to yield a material suitable to study the influence of stacking fault defects on the Raman spectrum. X-ray-diffraction measurements revealed that the films consist of randomly oriented 3*C*-SiC crystallites.[10,11] The microcrystalline morphology was confirmed by scanning electron microscopic images which show particles of about 100-nm size. We have measured the heat conductivity of this microcrystalline material to be a factor of 20 smaller than that of single-crystalline 3*C*-SiC, and ascribed the low heat conductivity to the scattering of acoustical phonons at grain boundaries.[12]

For Raman measurements, a square-shaped window of 3×3-mm^2 size was etched into the silicon substrate in order to manufacture a free-standing SiC film. Due to thermal decoupling from the substrate in conjunction with the low value of the heat conductivity, we were able to heat the free-standing film to temperatures as high as 1700 K in the focus of a laser beam. For that purpose an argon-ion laser operating at 514.5 nm with a power up to 180 mW was focused to a spot of 18 μm in diameter.

Stokes and anti-Stokes Raman spectra were recorded in backscattering configuration with the same laser. The temperature was calculated from the ratio of Stokes and anti-Stokes intensities of the LO-phonon lines.[13]

For some of the measurements reported here, we used a Raman microprobe setup to record spectra with a spatial resolution of around 1 μm. These spectra were taken with low laser intensity ($\leqslant 5$ mW), so that the influence of heating in the laser focus could be neglected.

III. RESULTS AND DISCUSSION

Raman spectra were recorded for temperatures between room temperature and 1700 K by varying the laser power

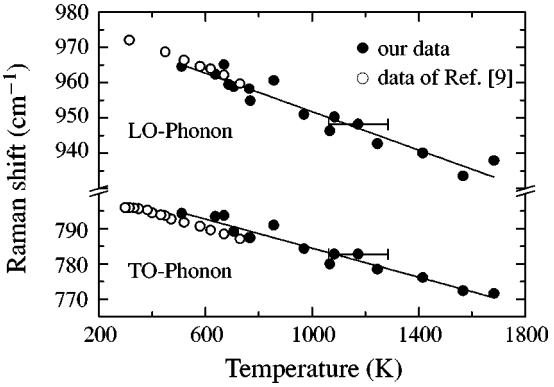

FIG. 1. Temperature dependence of LO and TO Raman lines for our samples (filled circles) and for single crystal 3*C*-SiC (open circles) from Ref. 9.

between 5 and 180 mW. The peak position and width [full width at half maximum (FWHM)] were determined for the LO- and TO-phonon lines, and are plotted in Figs. 1 and 2, respectively, as functions of temperature. A softening of the phonon frequencies with increasing temperature is observed for both modes. Data of Ref. 9 measured for single-crystalline 3*C*-SiC in a limited temperature range ($T<750$ K) are also shown in Fig. 1 for comparison. Good agreement for the temperature dependence of the peak positions is observed in the region of overlap in spite of the different sample morphologies. However, the linewidths (Γ), as shown in Fig. 2, differ significantly for the two samples, i.e., the linewidths of our polycrystalline 3*C*-SiC are considerably larger than those of single crystals, both for the LO and the TO lines. Taking three- and four-phonon processes into account, the temperature dependence of Γ is given theoretically by[14–17]

$$\Gamma^2(T)=\left[A\left(1+\frac{2}{e^x-1}\right)+B\left(1+\frac{3}{e^y-1}+\frac{3}{(e^y-1)^2}\right)\right]^2+\Gamma_1^2, \tag{1}$$

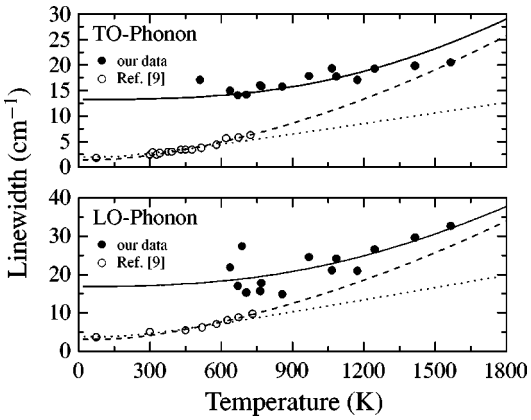

FIG. 2. Temperature dependence of the TO and LO Raman linewidths. The dotted line is a least-squares fit to the data of Ref. 9 considering three-phonon processes only [$B=0$ in Eq. (1)], whereas the solid and dashed lines are least-squares fits under inclusion of four-phonon processes for the data of Ref. 9 and our data, respectively.

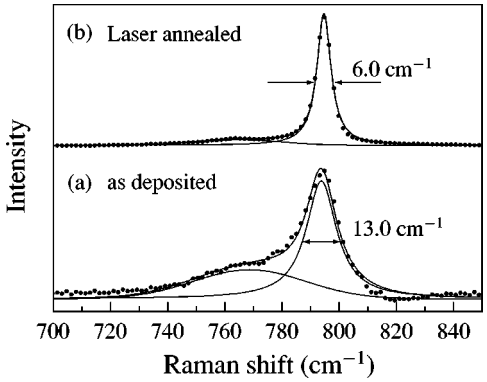

FIG. 3. TO Raman line before (a) and after (b) laser annealing at 1900 K. Both spectra were measured at room temperature.

where $x=\hbar\Omega_{\mathrm{LO,TO}}/2k_BT$, $y=\hbar\Omega_{\mathrm{LO,TO}}/3k_BT$, $\Omega_{\mathrm{LO,TO}}$ are the LO and TO frequencies, and A and B are constants. The first and second terms include the effect of three- and four-phonon processes on Γ, respectively. Whereas the terms in the brackets are an increasing function of temperature, Γ_1 is a temperature-independent contribution to the linewidth. Olego and Cardona[9] undertook temperature-dependent measurements of the phonon linewidth in single-crystalline 3*C*-SiC that could be described with Eq. (1) using $A=2.0$ and 3.8 cm^{-1} for the TO and LO lines, respectively, by neglecting four-phonon processes, i.e., $B=0$. The corresponding fit is the dotted line in Fig. 2. We find, however, that the fit to their data is slightly improved by inclusion of four-phonon processes with A and B equal to 1.21 and 0.27 cm^{-1} for the TO mode, and 2.68 and 0.44 cm^{-1} for the LO mode, respectively (dashed line in Fig. 2). It is obvious from Fig. 2 that four-phonon processes give an increasingly important contribution to $\Gamma(T)$ at temperatures above 750 K, the temperature range of our measurements. The importance of four-phonon processes was also pointed out in Ref. 18.

In contrast to the data of Ref. 9, an additional temperature-independent contribution Γ_1 has to be considered for our data as well. To determine Γ_1 we used A and B as obtained from the fit to the data of Ref. 9, and subsequently adjusted Γ_1 to yield the best agreement with our measurements (solid line in Fig. 2). The result is $\Gamma_{1,\mathrm{TO}}=13.1$ cm^{-1} and $\Gamma_{1,\mathrm{LO}}=16.6$ cm^{-1}.

During our measurements we gradually increased the laser power to reach temperatures up to 1900 K. At that temperature an irreversible change of the Raman spectrum occurs, as demonstrated in Fig. 3. The main features in the wave-number range shown are the TO line of 3*C*-SiC located at 795 cm^{-1}, and a second broader line centered at 766 cm^{-1}. The linewidth of the TO line is reduced from 13 to 6 cm^{-1} upon annealing, and the broader line is strongly reduced in intensity. Since that second peak does not show up in single-crystalline 3*C*-SiC, we conclude that this feature is related to crystalline imperfections and that the annealing at $T\geqslant 1900$ K improves the 3*C*-SiC crystal morphology.

We increased the laser power to a level sufficient that, eventually, a hole was burned into the film. Raman spectra were then recorded at room temperature at various distances from the center of that hole corresponding to a transition from the laser-annealed material to the as-deposited film.

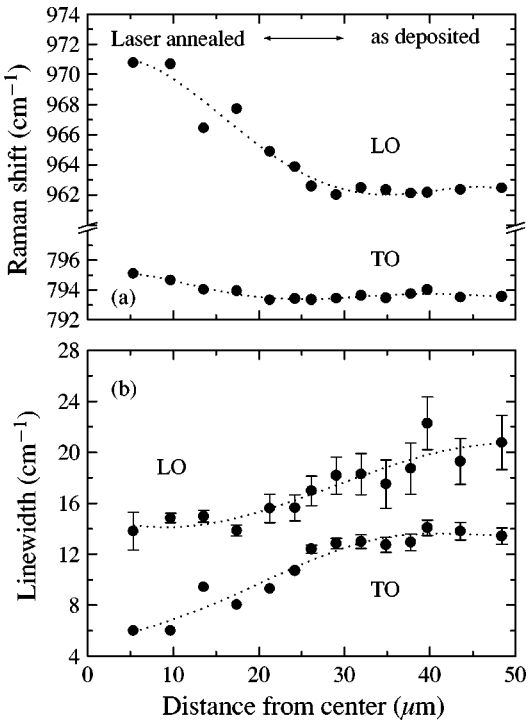

FIG. 4. Peak positions (a) and linewidths (b) of the TO and LO Raman lines after laser annealing. The laser power was chosen so as to burn a small hole into the free-standing SiC film. Data of micro-Raman measurements are plotted as a function of the distance from the center of the hole. The dotted lines through the experimental data have been drawn as a visual guide.

The center frequency and the linewidth of TO and LO lines are given as a function of spatial position in Figs. 4(a) and 4(b), respectively. Both lines shift to higher frequencies due to the laser annealing and narrow at the same time.

Different alternatives have been discussed to account for a broadening of phonon lines such as nonuniform heating in the laser focus,[19] phonon confinement in nanocrystals,[15,20] or lattice imperfections.[16] For our measurements the effect of nonuniform heating can be excluded, since the broadening of the phonon lines persists at room temperature, and even at higher laser power a broadening due to inhomogeneous temperature distribution is negligible.[21]

Due to momentum conservation in single crystals only phonon modes with a wave vector k close to the center of the Brillouin zone (BZ) contribute to Raman scattering. In the phonon confinement model broadening is ascribed to the relaxation of the $k=0$ selection rule in small crystallites when vibrational modes away from the BZ center contribute to Raman scattering.[15,20] To account for the measured value of Γ_1 crystallite sizes of about 1 nm would be required, much smaller than the 100 nm size observed in scanning electron microscope images. Thus we exclude phonon confinement as the main effect. Sasaki *et al.*, in a similar situation, discussed an extra anharmonicity at internal defects as the reason for their observed line broadening.[16]

In the following we adopt the idea of Nakashima *et al.*, who considered polytype disorder in SiC crystals as an origin for phonon line broadening.[8] For perfect SiC polytypes they found quantitative agreement between calculated and measured Raman intensity profiles using the bond polarizability

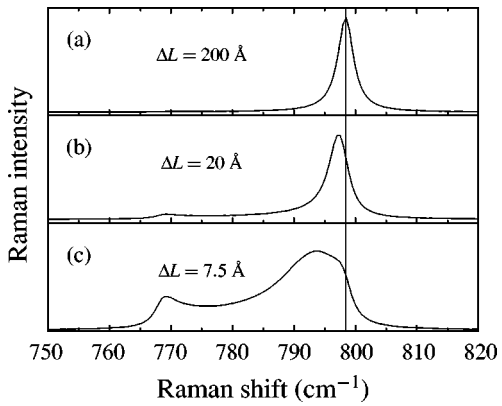

FIG. 5. Raman spectra of the TO mode simulated with the bond polarizability model for 3C-SiC with randomly distributed stacking faults. Average stacking fault distances are $\Delta L = 200$ Å (a), 20 Å (b), and 7.5 Å (c). For reference, the vertical line marks the TO line position for crystalline 3C-SiC.

model. In this model, the total polarizability that is responsible for the emission of scattered light is obtained as the sum of the contributions from the bond Raman polarizabilities multiplied by the bond-length variation associated with a given phonon mode. For SiC polytypes, the bond Raman polarizabilities can be approximately expressed by a single parameter with fixed magnitude describing the bonds in each Si-C double layer. The sign of the polarizability depends, however, on the bond orientation. Double layers with a cubic stacking have the same sign, whereas hexagonal stacking reverses the sign of polarizability.[7] Consequently, each polytype has a characteristic sequence of bond polarizability, e.g. $(+++---)$ in 6H-SiC or $(++++\cdots)$ in 3C-SiC. Nakashima *et al.* also applied that model to calculate the Raman intensity profiles in disordered structures. They showed that structures with a random distribution of domains of different polytypes exhibit a broadening and distortion of the Raman lines.[8]

In the present paper, we consider a 3C-SiC crystal that has a random sequence of stacking faults in the (111) direction normal to the Si-C double layers with a concomitant change in the sign of the bond polarizability at each stacking fault. The disorder is thus one dimensional. To estimate the influence of stacking faults on the line shape in Raman spectra, series of 1000 Si-C double layers with stacking faults were simulated with a computer. Poisson distributions were taken for the probability to find stacking faults with the mean stacking fault distance ΔL as the characteristic parameter. For the calculation the sequence of 1000 double layers was repeated periodically; in other words, an artificial polytype with a period of 1000 double layers was generated. The Raman profile of the TO phonon line was then calculated with the algorithm of Nakashima and co-workers,[5,8] and folded with a natural linewidth of 3C-SiC. We averaged 200 of such simulated Raman spectra for each choice of ΔL.

Representative spectra calculated for three such random structures with different ΔL are shown in Fig. 5. The TO line shifts to lower frequencies and broadens with decreasing ΔL, i.e. with increasing disorder. The peak position and the width (FWHM) derived from such simulated spectra are plotted as a function of ΔL in Figs. 6(a) and 6(b), respectively. For $\Delta L > 20$ Å the down shift is smaller than 1 cm^{-1},

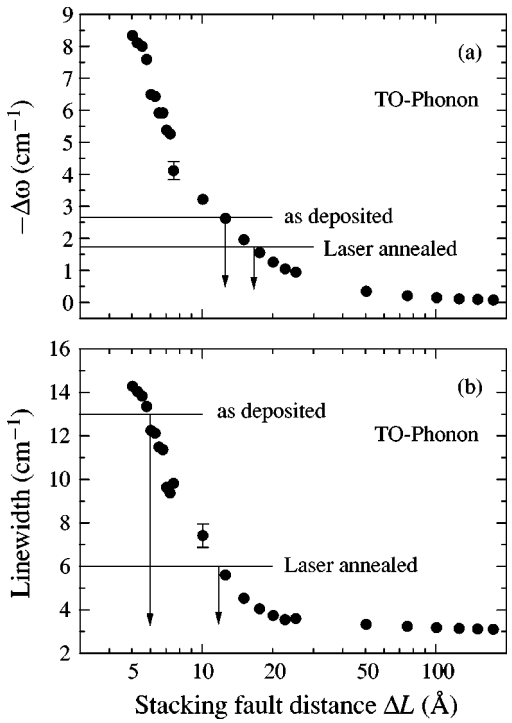

FIG. 6. (a) Simulated peak shift relative to that of single crystalline SiC of the 3*C*-SiC TO Raman line vs average stacking fault distance ΔL. Using the experimentally determined peak shifts ΔL, values of 13 and 17 Å are obtained for the as-deposited and the annealed film, respectively. (b) Simulated linewidth of the 3*C*-SiC TO Raman line vs average stacking fault distance ΔL. The measured linewidths of 13 and 6 cm^{-1} (Fig. 5) yield 6 and 12 Å for ΔL, respectively, as marked with arrows.

and the line is only negligibly broadened. The effect of shifting and broadening becomes significant, however, when ΔL is reduced below 20 Å. At the same time a shoulder appears at 768 cm^{-1}, with an intensity that increases with decreasing average stacking fault distance. The mean frequency of the shoulder corresponds roughly to that of the zone edge TO phonon of 3*C*-SiC. We shall interpret this observation below by comparing the phonon confinement model with our model of stacking disorder.

Using the variation of line position and width with ΔL, we estimate the degree of disorder in our samples. The experimental values are marked in Figs. 6(a) and 6(b). The experimentally observed linewidths [Fig. 6(b)] would correspond to stacking fault distances of $\Delta L \approx 6$ and 12 Å for the as deposited and annealed sample, respectively, while the peak shifts $\Delta\omega$ [Fig. 6(a)] yield somewhat larger values of 13 and 17 Å. We believe that these discrepancies are mainly due to the linear chain model, which is unable to give the phonon frequencies with a precision better than about 2 cm^{-1}. The influence of the stacking sequence on the phonon frequencies, that was experimentally observed in polytypes,[22] will consequently affect the evaluation of ΔL from the peak position [Fig. 6(a)] more strongly than evaluation from the linewidth [Fig. 6(b)]. We thus regard the values of 6 and 12 Å for the as-deposited and annealed sample to be more reliable. Stacking faults have been observed directly in the past by scanning transmission electron microscopy in SiC whiskers

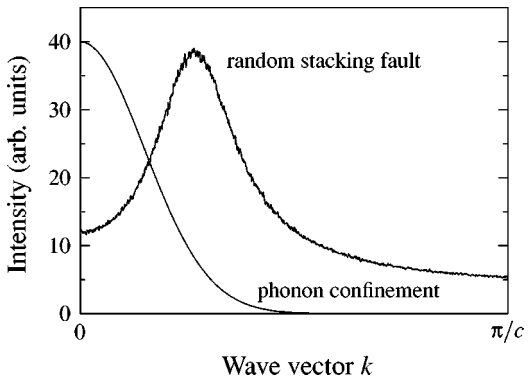

FIG. 7. Comparison of the Raman intensity vs wave-vector relationship in the random stacking fault and the phonon confinement model, respectively. We have used $\Delta L = 7.5$ Å as the average distance between stacking faults. The crystalline size for the phonon confinement model was also assumed to be 7.5 Å.

with spacings of 20–200 Å,[23] and recently in heteroepitaxially films of 3*C*-SiC grown on silicon.[24]

Circumstantial support for our model comes from the annealing behavior of our samples. By increasing the temperatures above 1900 K the TO line narrows irreversibly, and the shoulder on the lower-frequency side clearly visible in Fig. 3(a) nearly disappears. This would imply an annealing of stacking faults in 3*C*-SiC at that temperature. It is intriguing that the annealing of stacking faults occurs at a temperature where 2*H*-SiC transforms to 3*C*-SiC,[25] a transformation that also requires a switching in the bond direction. The transformation is likely to be fostered by the small grain size of our microcrystalline samples.

In the following we discuss the physical origin of the TO Raman line broadening due to disorder by comparing the phonon confinement model and our random stacking fault model. The basic effect is the same in both models: The TO-phonon branch disperses in the Brillouin zone. Its vibrational frequency is highest at the Γ point ($k=0$), and is monotonical reduced toward the Brillouin zone edge. As mentioned above, only modes with $k=0$, i.e. the highest frequency modes in the branch, are observable in Raman spectra of single-crystalline 3*C*-SiC. Consequently, any relaxation of the $k=0$ selection rule will make only lower-lying modes accessible, implying a broadening toward lower frequencies. In the phonon confinement model the contribution of modes to the Raman spectrum is calculated by assuming a Gaussian distribution function of phonon states in k space:

$$I^{\Delta l}(k) = I_0 \exp(-k^2 \Delta l^2/4). \tag{2}$$

The width of that distribution is inversely proportional to the crystalline size Δl and, hence, a contribution of phonon modes away from the zone center give the observed broadening and downshift.[15,20]

In the random stacking fault model no similar explicit assumption is made about the relative contribution of vibrational modes, but we confirmed the effect of $k \neq 0$ modes as the reason for line broadening in our calculations by inspecting the corresponding $I^{\Delta L}(k)$ relationship.

In Fig. 7 one example for $\Delta L = 7.5$ Å is plotted as a function of wave vector together with the corresponding relationship from Eq. (2) in the phonon confinement model with

$\Delta l = 7.5$ Å. Whereas the latter curve is centered at $k=0$, this is not the case for the random stacking fault model. Rather, a distribution centered at $k \approx 0.27\pi/c$ is observed, where c is the distance between double layers, accompanied by a significant contribution extending over the whole Brillouin zone. We checked that the peak position scales with $1/\Delta L$.

This observation can be interpreted as follows. Neglecting, for the time being, one-dimensional disorder, a bond switch after a distance ΔL corresponds to a polytype with a period $2\Delta L$. For such a polytype phonon modes with wave vectors k, according to

$$k_m = (2m+1)\frac{\pi}{\Delta L}, \quad m = 0,1,2\ldots, \tag{3}$$

are Raman active in the framework of the bond polarizability model. In particular the $k=0$ mode no longer contributes to the Raman scattering, and the first active mode is that with $k_0 = \pi/\Delta L$.

Since the structures that we have simulated here can be regarded as disordered polytypes with period $2\Delta L$, the selection rule according to Eq. (3) is relaxed, resulting in a broadening similar to the mechanism operative in the phonon confinement model with the difference that the k-vector relaxation is now centered about $k_0 \neq 0$. The expected broadening is indeed observed in Fig. 7.

The Raman intensity $I(\hbar\Omega)$ is connected with $I(k)$, and the phonon-dispersion relation $\hbar\Omega(k)$ according to

$$I(\hbar\Omega) = \frac{I(k)}{(d\Omega/dk)}. \tag{4}$$

As a result, the maxima in the one-dimensional phonon density of states at $k=0$ and $k=\pi/c$ emphasize contributions at the extreme frequencies of the phonon branch. The singularities are reduced due to folding with the natural linewidth of the Raman signal. This ''density-of-states'' effect is the reason for the observed peak at the lower limit of frequencies in the TO-phonon branch. Note that this is much more pronounced for the random stacking fault model compared with the phonon confinement model, when similar disorder is assumed (see Fig. 7).

IV. CONCLUSION

We have measured temperature-dependent Raman spectra of the TO- and LO-phonon lines in free-standing films of microcrystalline $3C$-SiC that were grown on silicon. The temperature dependence of the phonon frequencies agrees with that of single-crystal $3C$-SiC, but the linewidths are considerably larger. We demonstrate that the Raman lines narrow after laser-induced thermal annealing of the microcrystalline films. To explain the phonon line broadening, we have simulated $3C$-SiC with randomly distributed stacking faults in the (111) direction, and calculated its Raman spectrum in the framework of a bond polarizability model. Due to the disorder in bond polarizability, phonon modes with wave vectors away from the center of the Brillouin zone become accessible to Raman scattering. We conclude that such a stacking disorder can be responsible for the line broadening measured in our films if the average distance between stacking faults is of the order of 6 Å, i.e., an average distance of 2–3 double layers.

ACKNOWLEDGMENTS

We would like to thank Dr. G. Müller and Dr. G. Krötz from Daimler-Benz AG for the samples. This work was supported by the Deutsche Forschungsgemeinschaft under Sonderforschungsbereich 292 Mehrkomponentige Schichtsysteme (MEKOS).

[1] R. F. Davis, Physica B **185**, 1 (1993).
[2] J. W. Palmour, J. A. Edmond, H. S. Kong, and C. H. Carter, Jr., Physica B **185**, 461 (1993).
[3] D. W. Feldman, J. H. Parker, Jr., W. J. Choyke, and L. Patrick, Phys. Rev. **170**, 698 (1968).
[4] D. W. Feldman, J. H. Parker, Jr., W. J. Choyke, and L. Patrick, Phys. Rev. **173**, 787 (1968).
[5] S. Nakashima, H. Katahama, Y. Nakakura, and A. Mitsuishi, Phys. Rev. B **33**, 5721 (1986).
[6] S. Nakashima, Y. Nakakura, and Z. Inoue, J. Phys. Soc. Jpn. **56**, 359 (1987).
[7] S. Nakashima and K. Tahara, Phys. Rev. B **40**, 6339 (1989).
[8] S. Nakashima, H. Ohta, M. Hangyo, and B. Palosz, Philos. Mag. B **70**, 971 (1994).
[9] D. Olego and M. Cardona, Phys. Rev. B **25**, 3889 (1982).
[10] G. Krötz *et al.*, Mater. Sci. Eng. B **29**, 154 (1995).
[11] G. Krötz (private communication).
[12] S. Rohmfeld, M. Hundhausen, and L. Ley, Mater. Sci. Forum **264–268**, 657 (1998).
[13] T. R. Hart, R. L. Aggarwal, and B. Lax, Phys. Rev. B **1**, 638 (1970).
[14] M. Balkanski, R. F. Wallis, and E. Haro, Phys. Rev. B **28**, 1928 (1983).
[15] H. Richter, Z. P. Wang, and L. Ley, Solid State Commun. **39**, 625 (1981).
[16] Y. Sasaki, Y. Nishina, M. Sato, and K. Okamura, Phys. Rev. B **40**, 1762 (1989).
[17] Equation (1) is a combination of formulae given by other authors. Reference 14 considers single-crystalline material and shows the importance of four-phonon processes. References 15 and 16 discuss linewidths for microcrystalline materials but without considering four-phonon processes.
[18] H. Harima, T. Hosoda, and S. Nakashima, Mater. Sci. Forum **264–268**, 449 (1998).
[19] H. W. Lo and A. Compaan, J. Appl. Phys. **51**, 1565 (1980).
[20] K. K. Tiong, P. M. Amirtharaj, F. H. Pollak, and D. E. Aspnes, Appl. Phys. Lett. **44**, 122 (1984).
[21] We estimate a broadening of no more than 2 cm^{-1} due to the inhomogeneous temperature distribution across the laser spot.
[22] S. Nakashima and H. Harima, Phys. Status Solidi A **162**, 39 (1997).
[23] J. F. DiGregorio, T. E. Furtak, and J. J. Petrovic, J. Appl. Phys. **71**, 3524 (1992).
[24] K. Yagi and H. Nagasawa, Mater. Sci. Forum **264–268**, 191 (1998).
[25] Y. Sasaki, Y. Nishina, M. Sato, and K. Okamura, J. Mater. Sci. **22**, 443 (1987).